MECHANICS AND MECHANICAL ENGINEERING
International Journal
Vol. 3 No. 1 1999

DYNAMICS OF THE LINEAR OSCILLATOR WITH IMPACTS

Krzysztof Czołczyński, Barbara Błażejczyk-Okolewska
Technical University of Łódź
Division of Dynamics
Stefanowskiego 1/15, 90-924 Łódź, Poland
E-mail: dzanta@ck-sg.p.lodz.pl

Abstract

A dynamical behaviour of the linear oscillator with one degree of freedom is presented. During a motion excited by an external harmonic force the oscillator impacts on the basement. A physical and mathematical model of the system, as well as bifurcation diagrams showing an effect of the excitation frequency on the character of the system motion have been discussed. Results of the analysis of an influence of the viscous damping coefficient on regularity of the oscillator motion have also been presented. The investigations have been conducted by means of numerical simulations.

Introduction

Mechanical systems whose elements impact on one another during operation have been extensively investigated by researchers. The reason of this interest lies in the fact that impacts occur very often in many modern technical devices. The phenomenon of impact is either desirable, being the basis of their operation, as in e.g. pneumatic hammers, impact print hammers [10] and heat exchangers [3, 1], or is destructive and should be eliminated, as in e.g. gear-boxes [5].

Early studies of impact oscillators, carried out by Peterka [7, 8], comprised some numerical investigations. More recent studies were initiated by Shaw and Holmes [9] and Foale and Bishop [2]. In their works, tools of modern nonlinear dynamics have also been applied. One of fundamental works devoted to the dynamical behaviour of a one-degree-of-freedom oscillator with impacts is the study by Nordmark [6], in which a survey of modern methods used for modelling systems with impacts and analysis of their motion, a grazing incidence as a reason of a nonperiodic motion in an impact oscillator, effects of a low velocity impact, and also a comparison between numerical and experimental results have been presented.

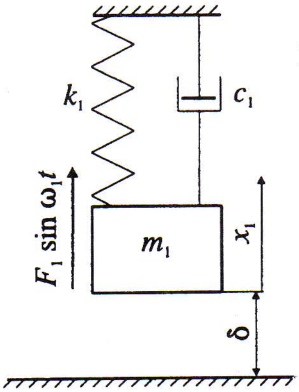

Figure 1. Oscillator in static equilibrium position.

Dynamics of oscillators with impacts has also been studied by Hinrichs, Oestreick and Popp [4]. They have presented a comparison of the results of experimental investigations with the results of numerical simulations concerning the mathematical model in which the Newton's law has been employed to describe impacts, and they have also presented a method for determination of the Lyapunov exponent in nonsmooth systems.

The investigations presented below have been devoted to analysis of vibrations of a linear oscillator with one degree of freedom. These vibrations have been caused by an external harmonic exciting force and impacts of the oscillator on the basement.

A special attention has been paid to determination of effects of the exciting force frequency and the viscous damping coefficient on regularity of the system motion. The investigations have been carried out by means of numerical simulations of the motion of the mathematical model of the system. Owing to advantageous results of the comparison shown in [4], the effect of impact has been modelled using the Newton's law.

Mathematical Model of the System

The sustem under considerations is the linear oscillator with one-degree-of-freedom, presented in Figure 1. When there is no contact between the oscillator and the basement, the motion of the system is described by the well known equation:

$$m_1 \frac{d^2 x_1}{dt^2} + c_1 \frac{dx_1}{dt} + k_1 x_1 = F_1 \sin \omega_1 t \tag{1}$$

where m_1 is the mass of the oscillator, c_1 - coefficient of viscous damping, k_1 - stiffness coefficient of massless spring, F_1 - amplitude of forcing, and ω_1 - frequency of forcing. Dividing equation (1) by k_1 and by the static deflection $x_{1st}=F_1/k_1$, and introducing the normalized time

$$\tau = \alpha_1 t \ , \quad \text{where} \quad \alpha_1^2 = \frac{k_1}{m_1} \ , \tag{2}$$

we obtain equation (1) in the form

$$\ddot{x}_1 + 2\gamma_1 \dot{x}_1 + x_1 = q_1 \sin\eta_1 \tau \tag{3}$$

where

$$q_1 = \frac{F_1}{k_1 x_{1st}}, \quad \eta_1 = \frac{\omega_1}{\alpha_1}, \quad \gamma_1 = \frac{c_1}{2\sqrt{k_1 m_1}},$$

$$\dot{x}_1 = \frac{dx_1}{d\tau} = \frac{1}{\alpha_1}\frac{dx_1}{dt}, \quad \ddot{x}_1 = \frac{d^2 x_1}{d\tau^2} = \frac{1}{\alpha_1^2}\frac{d^2 x_1}{dt^2}. \tag{4}$$

Symbol γ_1 denotes the relation between the actual damping and the critical one. In many cases it is more easy to give a value of the logarythmic decrement of damping Δ_1 (equal to a natural logarythm of a relation of two subsequent amplitudes of free vibrations). The relationship between γ_1 and Δ_1 is as follows:

$$\gamma_1 = \frac{\Delta_1}{\sqrt{4\pi_2 + \Delta_1^2}}. \tag{5}$$

Equations describing the impact, based on the well known Newton's law base are as follows:

$$m_1 \left(\frac{dx_1}{dt}\right)' - m_1 \frac{dx_1}{dt} = S_d, \quad \left(\frac{dx_1}{dt}\right)' = -k_r \frac{dx_1}{dt}, \tag{6}$$

and after dividing by $m_1 \alpha_1$ may be writter in the dimensionless form

$$\dot{x}_1' - \dot{x}_1 = S, \quad \dot{x}_1' = -k_r \dot{x}_1. \tag{7}$$

Additionally δ is the distance between the base and the colliding surface of the oscillator (delated to x_{1st}).

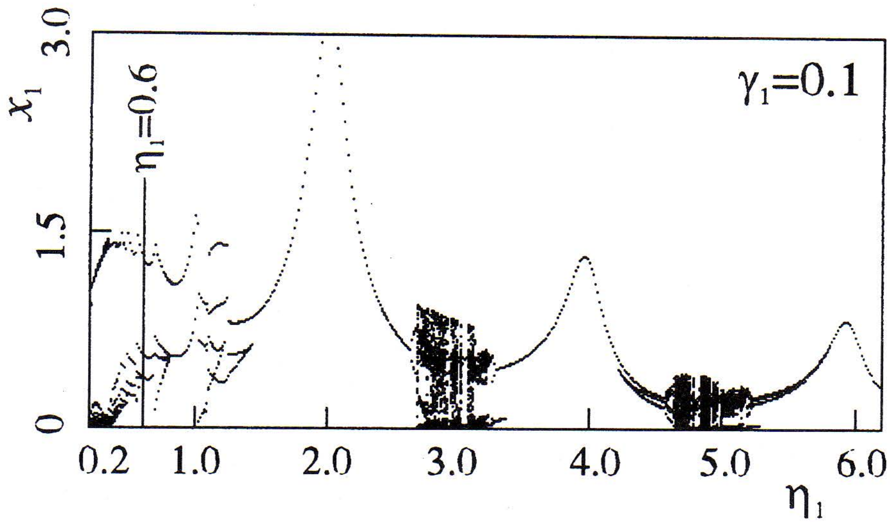

Figure 2. Resonance diagram of the oscillator, γ_1=0.1.

Influence of the Exciting Force on the Dynamical Behaviour of the System

The object under investigation is an oscillator to which a harmonic force with the amplitude q_1 = 1.0 m corresponding to the stiffness coefficient k_1 has been applied. The static equilibrium position is determined by the parameter δ = 0.01 m. The restitution coefficient k_r = 0.9.

Figure 2 shows a resonance diagram plotted for the system under consideration with the damping coefficient assumed to be γ_1 = 0.1 (with respect to the critical damping). The dimensionless frequency η_1 of the exciting force is presented on the horizontal axis, whereas the vibration amplitudes determined as system deflections at the instants when the system velocity equals zero are shown on the vertical axis.

As can be easily observed, the system under analysis is characterised by occurrence of superharmonical resonances in the neighbourhood of η_1 = 2, 4, 6, ... In the vicinity of these values of η_1 the system motion is regular, and the vibration amplitudes reach local extreme values.

Figure 3a shows a time diagram of the system motion for η_1 = 2.5. Additionally, a qualitative time history of the exciting force (upper, sinusoidal line) has been plotted on this diagram. As can be seen, the system motion is regular with period 1: one motion cycle occurs per one period of the exciting force. In the neighbourhood of remaining superresonance frequencies, the system motion is regular as well, with period 2 ($\eta_1 \approx$ 4) and 3 ($\eta_1 \approx$ 6), respectively, which means that one motion cycle occurs per two or three periods of the exciting force. The confirmation of this observation is to be found

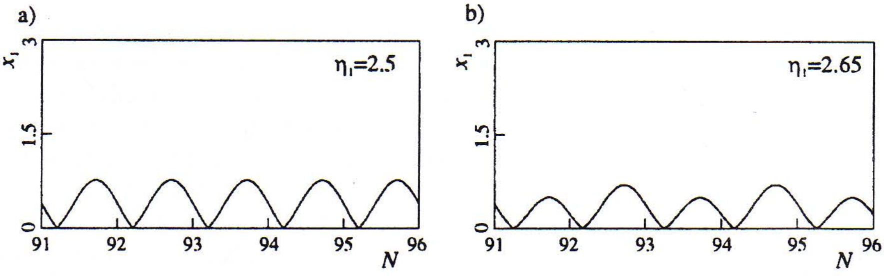

Figure 3. Time diagram of the motion, γ_1=0.1.

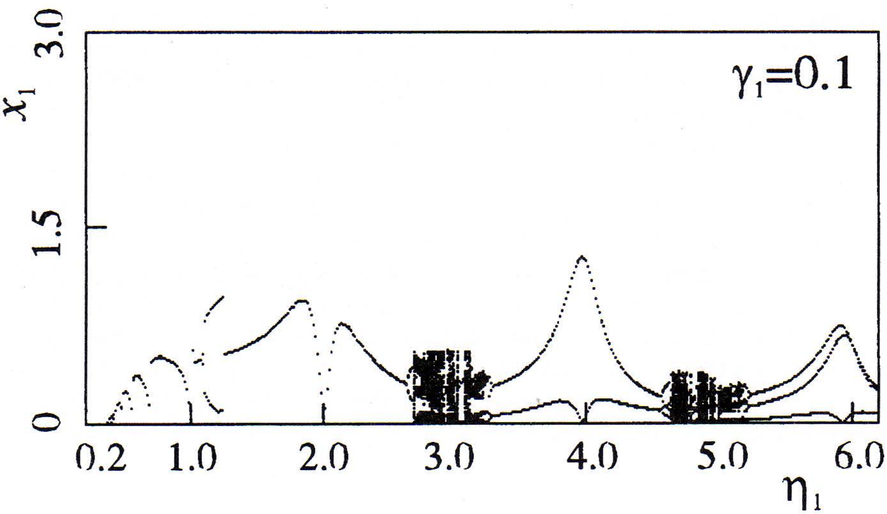

Figure 4. Bifurcation diagram of the oscillator, γ_1=0.1.

in Fig. 4 which is a classical bifurcation diagram: displacements of the system at the instants distant from each other by one period of the exciting force are presented on the vertical axis. On this diagram, one can see one (period one, $\eta_1 \approx 2$), two (period two, $\eta_1 \approx 4$) or three (period three, $\eta_1 \approx 6$) lines, respectively, in the vicinity of superharmonic resonances.

As has been shown in Figs. 2 and 4, the second characteristic feature of the system under analysis is occurrence of regions of a chaotic motion when the exciting force frequency is close to 3 and 5.

The reason underlying occurrence of a chaotic motion in these regions is easy to understand if one observes the time diagram plotted for $\eta_1 = 2.7$ (Fig. 5). As can be seen, at distances equal to 3 periods of the exciting force, the exciting force acting

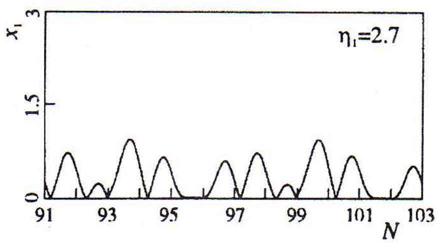

Figure 5. Time diagram of the motion, γ_1=0.1.

upwards (and thus impeding the system) reduces the oscillator velocity to the value equal to almost zero (or exactly equal to zero) just before impact, and then it "holds" the oscillator in the neighbourhood of the basement. As a result of such behaviour of the exciting force, an impact does not occur at all or a few impacts with small velocities take place (grazing effect), which causes irregular (chaotic) behaviour of the system. This character of the motion is confirmed by the phase portrait and Poincare map shown in Fig. 6. The transition from a regular motion (in the vicinity of $\eta_1 \approx 2, 4, 6$) into an irregular one (in the neighbourhood of $\eta_1 = 3, 5$) is accompanied by the phenomenon of period doubling, which can be seen on the time diagram presented for $\eta_1 = 2.65$ in Fig. 3b.

Figure 7 depicts a resonance diagram of the system (analogue to that shown in Fig. 2) in the range $0.2 < \eta_1 < 1.2$. Nonsmoothness on the plots of amplitudes observed on this diagram is caused by a change in the "rhythm" of the system operation, resulting from a change in the exciting force frequency. For instance, for $\eta_1 = 0.3$, a period of the exciting force is long enough for the oscillator to come into a continuous contact with the basement after a sequence of impacts occurring one after another (time diagram in Fig. 8a). At higher values of η_1, one can observe 5 impacts ($\eta_1 = 0.45$, Fig. 8b), 4 impacts ($\eta_1 = 0.5$, Fig. 8c), 3 impacts ($\eta_1 = 0.6$, Fig. 8d), etc., up to 1 impact ($\eta_1 = 1.05$, Fig. 8e) during one period of the exciting force. For $\eta_1 = 1.5$, (Fig. 8f) the vibration characteristic curve is already similar to that observed for the first superharmonic resonance (Fig. 3).

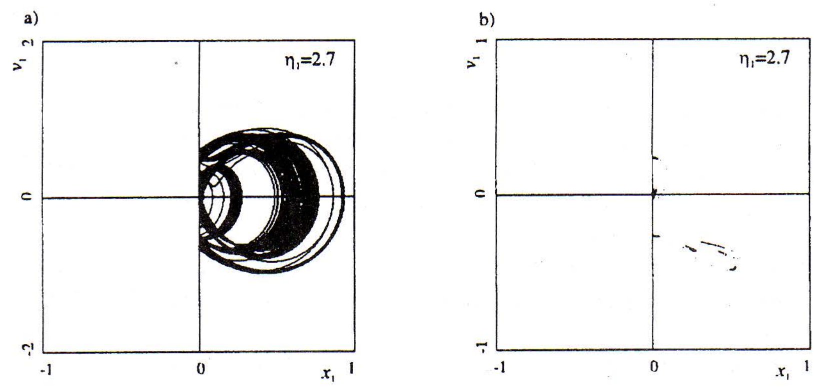

Figure 6. Phase plane and Poincare map, η_1=2.75, γ_1=0.1.

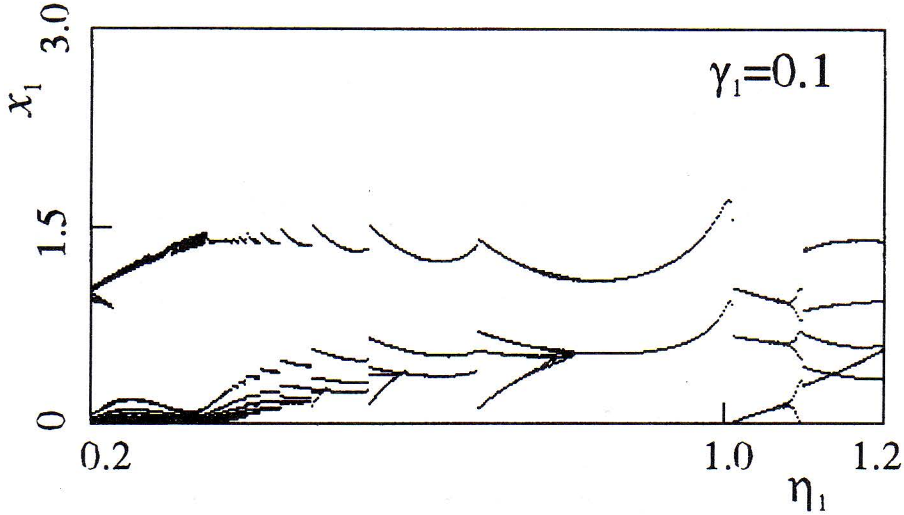

Figure 7. Resonance diagram of the oscillator, γ_1=0.1.

Influence of the Damping Coefficient on the System Behaviour

Figures 9, 2 and 10 show the resonance diagrams for various values of the damping coefficient γ_1. As can be seen, an increase in the damping coefficient is followed by disappearance of regions of a chaotic motion in the subresonance range ($\eta_1 < 1$). This phenomenon can be observed in Fig. 11 showing the bifurcation diagram plotted for $\eta_1 = 0.6$, on the assumption that the damping coefficient γ_1 is the bifurcation parameter. A chaotic motion changes into a regular one for $\gamma_1 > 0.06$, whereas for $\gamma_1 > 0.4$ a periodic continuous contact of the oscillator with the basement is observed.

A comparison of Figs. 9, 2 and 10 points out that regions of a chaotic motion occurring in the neighbourhood of the exciting force frequency $\eta_1 \approx 3$ and $\eta \approx 5$ disappear for high values of the damping coefficient as well.

On the other hand, however, an increase in the damping coefficient leads to a decrease in the amplitude of free vibrations initiated by impacts. When this amplitude is close to the amplitude of the vibrations excited by the harmonic exciting force, additional impacts in superharmonic resonance regions occur. A regular motion observed here so far changes into a chaotic one, owing to the grazing effect: cf. an example presented in Fig. 12 for $\gamma_1 = 0.6$ and $\eta_1 = 5.9$.

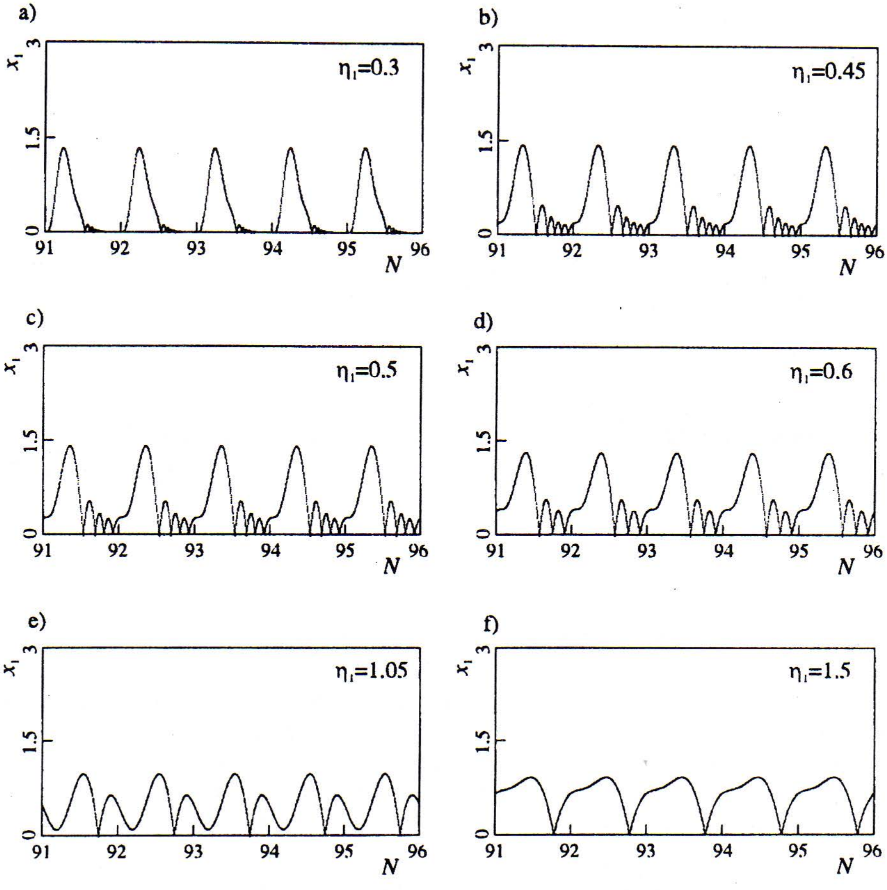

Figure 8. Time diagrams of the motion, γ_1=0.1.

Conclusions

The results of numerical investigations show that a motion of the oscillator impacting on the basement can be either regular or chaotic, depending on the exciting force frequency. The basic, largest regions of a regular motion are observed for the frequency of the exciting force close to even multiples of the free vibration frequency, whereas the regions of a chaotic motion occur at the exciting force frequency close odd multiples. The regions of a chaotic motion are reduced, or even disappear due to an increase in the value of the damping coefficient.

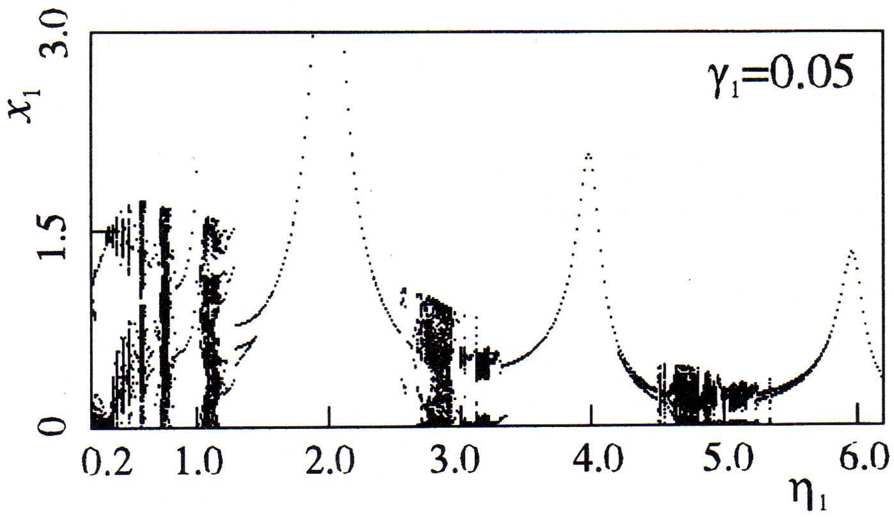

Figure 9. Resonance diagram of the oscillator, γ_1=0.05.

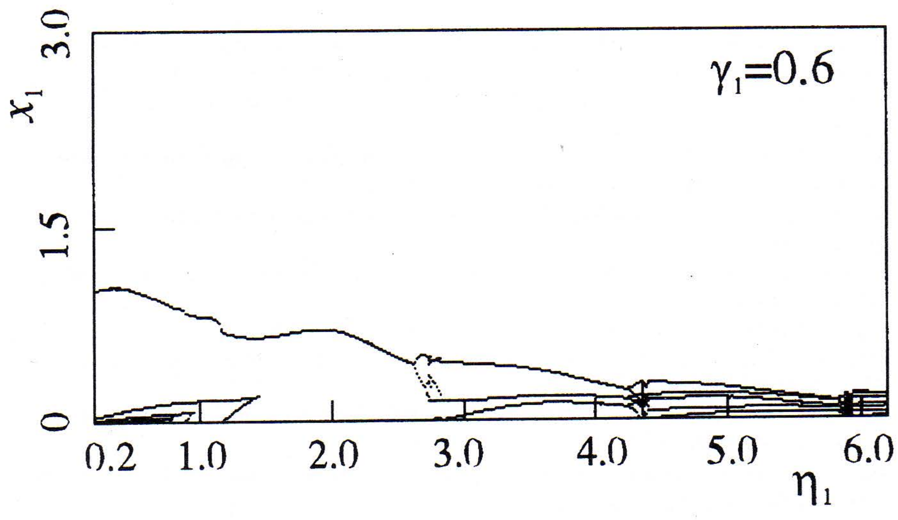

Figure 10. Resonance diagram of the oscillator, γ_1=0.6.

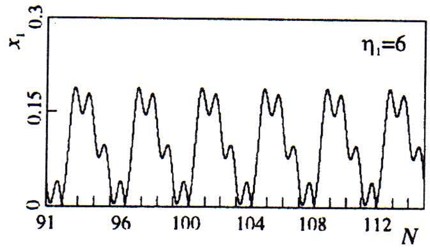

Figure 12. Time diagram of the motion, η_1=6, γ_1=0.6.

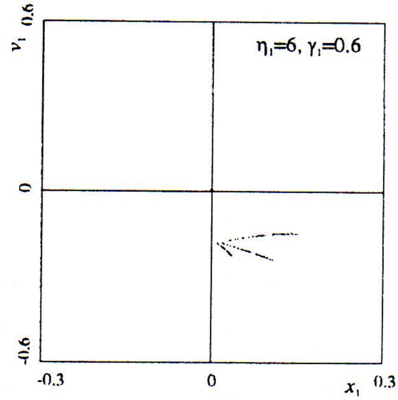

Figure 13. Poincare map, η_1=6, γ_1=0.6.

References

1. Blazejczyk-Okolewska B. and Czolczynski K.: Some aspects of the dynamical behaviour of the impact force generator. *Chaos, Solitons & Fractals*, **9**, 1998, 1307-1320.
2. Foale S. and Bishop S.R.: Dynamical Complexities of Forced Impacting Systems. *Philos. Trans. Royal Soc. London Ser. A*, **338**, 1992, 547-556.
3. Goyda H. and Teh C.A.: A Study of the Impact Dynamics of Loosely Supported Heat Exchanger Tubes. *ASME J. Pressure Tech.*, **111**, 1989, 394-401.
4. Hinrichs N., Oestreich M. and Popp K.: Dynamics of Oscillators with Impact and Friction. *Chaos, Solitons & Fractals*, **8**, 1997, 535-558.
5. Kaharaman A. and Singh R.: Nonlinear Dynamics of a Spur Gear Pair. *J. Sound Vibration*, **142**, 1990, 49-75.
6. Nordmark A.B.: Grazing Conditions and Chaos in Impacting Systems. Stockholm, 1992.
7. Peterka F.: Theoretical Analysis on *n*-multiple, (1/*n*)-impact Solutions, Part 1. *Acta Tech CSAV*, **19**, 1974, 462-473.
8. Peterka F.: Results of Analogue Computer Modelling of the Motion, Part21. *Acta Tech CSAV*, **19**, 1974, 569-580.
9. Shaw S.W. and Holmes P.J.: A Periodically Forced Piecewise Linear Oscillator. *J. Sound Vibration*, **90**, 1983, 129-155.
10. Tung P.C. and Shaw S.W.: The Dynamics of an Impact Print Hammer. *ASME J. Vibration Stress Reliability in Design*, **110**, 1988, 193-199.